

MultiNash-PF: A Particle Filtering Approach for Computing Multiple Local Generalized Nash Equilibria in Trajectory Games

Maulik Bhatt¹ Iman Askari² Yue Yu³ Ufuk Topcu⁴ Huazhen Fang² Negar Mehr¹

Abstract—Modern robotic systems frequently engage in complex multi-agent interactions, many of which are inherently multi-modal, i.e., they can lead to multiple distinct outcomes. To interact effectively, robots must recognize the possible interaction modes and adapt to the one preferred by other agents. In this work, we propose MultiNash-PF, an efficient algorithm for capturing the multimodality in multi-agent interactions. We model interaction outcomes as equilibria of a game-theoretic planner, where each equilibrium corresponds to a distinct interaction mode. Our framework formulates interactive planning as Constrained Potential Trajectory Games (CPTGs), in which local Generalized Nash Equilibria (GNEs) represent plausible interaction outcomes. We propose to integrate the potential game approach with implicit particle filtering, a sample-efficient method for non-convex trajectory optimization. We utilize implicit particle filtering to identify the coarse estimates of multiple local minimizers of the game’s potential function. MultiNash-PF then refines these estimates with optimization solvers, obtaining different local GNEs. We show through numerical simulations that MultiNash-PF reduces computation time by up to 50% compared to a baseline. We further demonstrate the effectiveness of our algorithm in real-world human-robot interaction scenarios, where it successfully accounts for the multi-modal nature of interactions and resolves potential conflicts in real-time.

I. INTRODUCTION

Many real-world robotic interactions are inherently multi-modal. For example, in the two-player interaction illustrated in Fig. 1, the agents need to move towards their goals while avoiding collisions. Here, two outcomes exist: both agents yielding to their right or left. If the two agents act independently, they might choose conflicting actions. For example, one yields to the left and the other to the right, which can potentially result in a collision. What trajectory each agent would prefer to pick depends on the *convention* they might be following. For example, in some cultures, in such settings, the convention is to yield to the right to avoid collisions, while in other cultures, the convention is to yield to the left. Such conventions typically emerge from repeated coordination problems [1], and autonomous agents must

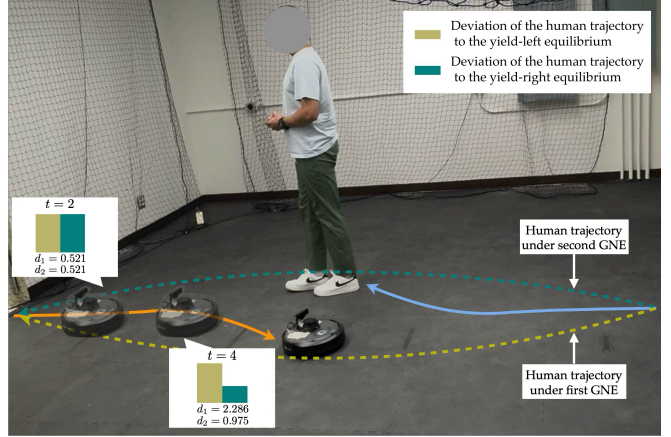


Fig. 1: Snapshot of an interaction between a robot and a human when they exchange positions. Using MultiNash-PF, the robot can compute both modes of interaction. At $t = 2$, the robot is uncertain about the preferred mode of the human since the human trajectory’s distance from both equilibria is almost the same. At $t = 4$, the human trajectory is closer to the yield-right GNE; therefore, the robot chooses the corresponding GNE and avoids collision with the human.

recognize them and account for the multi-modality of interactions to coordinate with humans effectively. Some recent works have shown that reasoning about the multi-modality of interactions is critical to aligning agents’ preferences over different outcomes [2] or helping coordinate agents’ actions via recommendation [3]. In this paper, we address this challenge by proposing MultiNash-PF, an algorithm that efficiently identifies multiple likely interaction outcomes in multi-agent domains and enables agents to adapt their plans accordingly.

We formulate the problem of computing multi-agent interaction outcomes as a multi-agent trajectory planning problem. To formalize interactions, we use dynamic game theory [4], which has been shown to be powerful in developing interactive and socially compliant robots [5], [6], [7], [8] where it has been shown that the interaction outcomes are captured through *generalized Nash equilibrium* (GNE). When multiple agents interact, a GNE corresponds to a joint action such that no agent has incentives to deviate from its equilibrium actions unilaterally. Several recent works have shown great success in utilizing GNE for modeling interaction outcomes in interactive domains [9], [10], [11], [12]. However, there typically exist multiple equilibria in interaction games, many of which are equally valid. We

¹Maulik Bhatt and Negar Mehr are with University of California, Berkeley, CA, 94720, USA {maulikbhatt,negar}@berkeley.edu

²Iman Askari and Huazhen Fang are with University of Kansas, Lawrence, KS, 66045, USA {askari,fang}@ku.edu

³ Yue Yu is with University of Minnesota, Minneapolis, 55455, USA yuey@umn.edu

⁴ Ufuk Topcu is with University of Texas at Austin, TX, 78712, USA utopcu@utexas.edu

This research involving human subjects was approved by the Committee for Protection of Human Subjects under Protocol No. 2024-11-18012.

This work was supported by the National Science Foundation, under grants ECCS-2438314 CAREER Award, CNS-2423130, and CCF-2423131.

argue that each equilibrium corresponds to a distinct *mode* of interaction. For instance, in Fig. 1, yielding to the right or left are both acceptable equilibria, representing different Nash equilibria. Consequently, we propose that in order to capture different interaction modes, robots must *reason about multiple interaction equilibria and select the one that aligns with the convention adopted by other agents*. However, this is a non-trivial task as it requires the robot to find all local GNEs. To our best knowledge, there is no principled approach to compute multiple local Nash equilibria in constrained trajectory games other than exhaustive random initializations of the game solvers.

In this paper, we tackle this challenge by introducing MultiNash-PF, a novel framework designed to efficiently compute multiple local GNEs in constrained trajectory games. This, in turn, enables robots to recognize and reason about multiple interaction modes. Our approach integrates 1) constrained potential games [13], a class of games for which local GNEs can be computed by solving a single constrained optimal control problem, and 2) constraint-aware implicit particle filtering which is a sample-efficient method recently applied to nonconvex trajectory optimization [14], to develop a principled approach for identifying various interaction outcomes.

Using CPTGs, we can compute a local GNE by minimizing the potential function of the game, which is equivalent to solving a single constrained optimal control problem. We can solve the resulting optimal control problem using off-the-shelf optimization solvers. Then, we use a constraint-aware implicit particle filtering method to identify multiple local minima of the potential minimization problem. This method eliminates the need for random initialization of the optimization solver by efficiently obtaining coarse estimates of different local GNEs. Next, we use the identified minima as initialization for an optimization solver to refine our solution. The solver then computes all the different local GNEs of the original game, which correspond to multiple modes of interaction among the agents. Leveraging the sample efficiency of the implicit particle filtering method, MultiNash-PF can explore and identify multiple local GNEs faster than random initialization of optimization solvers. We further show the real-time application of MultiNash-PF in a human-robot navigation setting where the robot can reason about the existence of different local GNEs and plan its motion autonomously based on the modality the human prefers.

II. RELATED WORKS

Game Theoretic Planning. Game-theoretic planning has been widely used for modeling interactive domains. One of the foundational works in game theoretic motion planning was [15]. A wide range of methods have been proposed to compute different types of equilibria such as Stackelberg equilibria [16], [7], Nash equilibria, and generalized Nash equilibria through techniques such as best response dynamics [17], [18], iterative linear-quadratic approximations [6], [10], [19], augmented Lagrangian-based solvers [20], and

potential games-based methods [13], [21], [11], [12], [22], [23]. However, the shortcomings of all these methods lie in the fact that they find only one Nash equilibrium of the underlying game and ignore the multi-modal nature of the problem that is crucial for coordination among agents. In [2], the authors recognize the existence of multiple equilibria and focus on inferring the equilibrium of other agents in the environment. However, their methodology relies on computing different approximate local Nash equilibria using rollouts of randomly selected initial strategies, which we show in this work performs poorly compared to our method.

Multiple Local Solutions to a Constrained Optimal Control Problem. Optimal control problems that are relevant to robotics are often nonconvex constrained optimization problems, which are solved using gradient-based methods such as interior-point algorithms [24] and sequential quadratic programming [25]. These methods, however, are limited to finding a single local solution per initialization. In the context of identifying all local GNEs, this limitation results in a significant computational burden as numerous initial guesses are required to explore the solution space. To address this, we depart from traditional approaches and adopt a Bayesian inference framework that enables simultaneous recovery of multiple local GNEs. Recent work [26], [27], [28] has demonstrated that constrained optimization problems can be reformulated as Bayesian inference tasks, enabling estimation algorithms to overcome the limitations of gradient-based solvers. In this setting, particle filtering methods [29], [30] provide a principled approach to capturing multimodal distributions. We leverage this by employing the implicit particle filter, which improves sample efficiency by focusing particles in high-probability regions of the posterior [31].

III. CONSTRAINED POTENTIAL TRAJECTORY GAMES

Let $\mathcal{N} := \{1, 2, \dots, N\}$ denote the set of agents' indices. We assume that the game is played over a finite time horizon of $\tau \in \mathbb{N}$ time-steps, where \mathbb{N} is the set of natural numbers. Let $x_t^i \in \mathbb{R}^{n_i}$ and $u_t^i \in \mathbb{R}^{m_i}$ denote the state and control input of the i -th agent at time t , respectively. We assume that the state of the i -th agent evolves as follows:

$$x_{t+1}^i = f^i(x_t^i, u_t^i), \quad (1)$$

for all $t \leq \tau$, where $f^i : \mathbb{R}^{n_i} \times \mathbb{R}^{m_i} \rightarrow \mathbb{R}^{n_i}$ is a continuously differentiable function characterizing the dynamics of the i -th agent. Let $n = \sum_{i=1}^N n_i, m = \sum_{i=1}^N m_i$. We denote the joint state, input, and dynamics of all agents as $x_t := [(x_t^1)^\top \ (x_t^2)^\top \ \dots \ (x_t^N)^\top]^\top$, $u_t := [(u_t^1)^\top \ (u_t^2)^\top \ \dots \ (u_t^N)^\top]^\top$, and $f := [(f^1)^\top \ (f^2)^\top \ \dots \ (f^N)^\top]^\top$ respectively. Note that each f^i is a vector-valued dynamics function for each agent. Therefore, $f : \mathbb{R}^n \times \mathbb{R}^m \rightarrow \mathbb{R}^n$ will be a vector-valued dynamics function for the joint system.

We assume that each agent has to satisfy some constraints that couple different agents' states and control inputs. Let $g : \mathbb{R}^n \times \mathbb{R}^m \rightarrow \mathbb{R}^c$ with $c \in \mathbb{N}$ denote a continuously differentiable function that defines the constraints on the joint state x_t and joint control input u_t at each time:

$$g(x_t, u_t) \leq 0_c, \quad (2)$$

where 0_c is a vector of zeros in \mathbb{R}^c . The aim of the constraint function g is to capture individual agents' strict preferences, such as each agent avoiding obstacles or avoiding collision with other agents. It should be noted that coupling amongst agents' decisions is captured through constraints.

We assume that each agent i aims to minimize an objective function. Let Q^i and Q_τ^i be positive semidefinite and R^i be positive definite matrices for all $i \in \mathcal{N}$. We assume that each agent i seeks to minimize the following objective:

$$\|x_\tau^i - \hat{x}_\tau^i\|_{Q_\tau^i}^2 + \sum_{t=0}^{\tau-1} \|x_t^i - \hat{x}_t^i\|_{Q^i}^2 + \sum_{t=0}^{\tau} \|u_t^i\|_{R^i}^2 \quad (3)$$

where $\hat{x}_t^i \in \mathbb{R}^{n_i}$ is the reference state for agent i at time t . Typically, the reference states for each agent is a path of minimum cost they would follow in the absence of other agents in the environment, e.g., a straight line connecting the start and goal location. Such a quadratic cost structure is a standard assumption in various motion planning domains [32]. Furthermore, we denote the joint reference state of all agents at time t as \hat{x}_t . We denote by $\text{blkdiag}(A_1, \dots, A_n)$ the block-diagonal matrix formed by placing matrices A_1, \dots, A_n on the diagonal with zeros elsewhere. Let $a_{0:\tau} := \{a_0, \dots, a_\tau\}$ denote the collection of vectors a_t 's over the entire horizon $0 \leq t \leq \tau$. We use $\{x_{0:\tau}^i, u_{0:\tau}^i\}_{i=1}^N$ to denote the joint trajectory of all N the agents at all times. Note that using the joint notation, we can equivalently write the joint trajectories of all agents as $\{x_{0:\tau}, u_{0:\tau}\}$.

A. Local Generalized Nash Equilibrium Trajectories

Due to the interactive nature of the problem, generally, it is not possible for all agents to minimize their costs simultaneously while satisfying the constraints. Therefore, the interaction outcome is best captured by *local GNE trajectories*. With dynamics as (1) and constraints as (2), we denote the game by

$$\mathcal{G} := (\mathcal{N}, \{Q^i\}_{i \in \mathcal{N}}, \{Q_\tau^i\}_{i \in \mathcal{N}}, \{R^i\}_{i \in \mathcal{N}}, g, f, \hat{x}_{0:\tau}).$$

For a given ϵ , we define the set of local trajectories around a joint trajectory as $\mathcal{D}(\{x_{0:\tau}, u_{0:\tau}\}, \epsilon) = \left\{ \{x'_{0:\tau}, u'_{0:\tau}\} \middle| \sum_{t=0}^{\tau} (\|x_t - x'_t\|_2^2 + \|u_t - u'_t\|_2^2) \leq \epsilon \right\}$. A local GNE trajectory for \mathcal{G} is then defined as follows.

Definition 1. A set of joint trajectories $\{x_{0:\tau}^{i*}, u_{0:\tau}^{i*}\}_{i=1}^N$ is a local GNE trajectory for \mathcal{G} if for every agent $i \in \mathcal{N}$, the agent's trajectory $\{x_{0:\tau}^{i*}, u_{0:\tau}^{i*}\}$ is an optimal solution of the following optimization problem within a local neighborhood $\mathcal{D}(\{x_{0:\tau}^*, u_{0:\tau}^*\}, \epsilon)$ for some $\epsilon > 0$:

$$\begin{aligned} \min_{\{x_{0:\tau}^i, u_{0:\tau}^i\}} & \|x_\tau^i - \hat{x}_\tau^i\|_{Q_\tau^i}^2 + \sum_{t=0}^{\tau-1} \|x_t^i - \hat{x}_t^i\|_{Q^i}^2 + \sum_{t=0}^{\tau} \|u_t^i\|_{R^i}^2 \\ \text{s.t. } & x_0^i = \hat{x}_0^i, \quad x_{t+1}^i = f^i(x_t^i, u_t^i), \quad 0 \leq t \leq \tau-1, \\ & g(\tilde{x}_t, \tilde{u}_t) \leq 0_c, \quad 0 \leq t \leq \tau, \end{aligned} \quad (4)$$

where we use the following notation in $g(\tilde{x}_t, \tilde{u}_t)$

$$\begin{aligned} \tilde{x}_t &:= [(x_t^{1*})^\top \ (x_t^{2*})^\top \ \dots \ (x_t^{i-1*})^\top \ (x_t^i)^\top \ (x_t^{i+1*})^\top \ \dots \ (x_t^{N*})^\top]^\top, \\ \tilde{u}_t &:= [(u_t^{1*})^\top \ (u_t^{2*})^\top \ \dots \ (u_t^{i-1*})^\top \ (u_t^i)^\top \ (u_t^{i+1*})^\top \ \dots \ (u_t^{N*})^\top]^\top. \end{aligned}$$

Intuitively, at a local GNE, no agent can reduce their cost function by independently changing their trajectory to any alternative feasible trajectory within the local neighborhood of the equilibrium trajectories. It is important to highlight that solving (4) requires solving a set of N coupled constrained optimal control problems, which is often computationally expensive. Therefore, finding all the local GNEs of the game can be time-consuming when using traditional game-theoretic methods that aim to solve coupled optimal control problems.

However, an important property of our trajectory game is that it is a potential game, i.e., a GNE of the original game can be computed by optimizing a single constrained optimal control problem called *Potential*, as described in [11]. This reduces the computational cost of computing the GNEs of the game. In the following, we will prove that game \mathcal{G} can be expressed as a constrained trajectory potential game and that any local minimizer of the potential function is a local GNE.

Theorem 1. A trajectory $\{x_{0:\tau}^{i*}, u_{0:\tau}^{i*}\}_{i=1}^N$ is a local GNE if within a local neighborhood $\mathcal{D}(\{x_{0:\tau}^*, u_{0:\tau}^*\}, \epsilon)$, it is an optimal solution of

$$\begin{aligned} \min_{\{x_{0:\tau}, u_{0:\tau}\}} & \|x_\tau - \hat{x}_\tau\|_{Q_\tau}^2 + \sum_{t=0}^{\tau-1} \|x_t - \hat{x}_t\|_Q^2 + \sum_{t=0}^{\tau} \|u_t\|_R^2 \\ \text{s.t. } & x_0 = \hat{x}_0, \quad x_{t+1} = f(x_t, u_t), \quad 0 \leq t \leq \tau-1, \\ & g(x_t, u_t) \leq 0_c, \quad 0 \leq t \leq \tau, \end{aligned} \quad (5)$$

for some $\epsilon > 0$, where $Q_\tau := \text{blkdiag}(Q_\tau^1, \dots, Q_\tau^N)$, $Q := \text{blkdiag}(Q^1, \dots, Q^N)$ and $R := \text{blkdiag}(R^1, \dots, R^N)$.

Proof. This theorem follows from [11, Thm. 2]. Since agent costs from (3) depend only on the individual agent's own states and control inputs, we use the results from [11, Thm. 2] to obtain the potential function of \mathcal{G} to be

$$\sum_{i=1}^N \left(\|x_\tau^i - \hat{x}_\tau^i\|_{Q_\tau^i}^2 + \sum_{t=0}^{\tau-1} \|x_t^i - \hat{x}_t^i\|_{Q^i}^2 + \sum_{t=0}^{\tau} \|u_t^i\|_{R^i}^2 \right). \quad (6)$$

Using the joint notations, we can re-write the sums in (6) as (5). Therefore, we have proven that \mathcal{G} is a CPTG with potential function (5). Hence, using Theorem 2 from [11], any local solution of (5) will also be a local GNE of \mathcal{G} . \square

Using Theorem 1, we want to find all local solutions of (5) that will also be local GNE trajectories as they correspond to different interaction modes and outcomes. We would like to acknowledge that finding local solutions of (5) will not necessarily give us all the GNEs of the original, as Theorem 1 provides only a sufficient condition for computing local GNEs. Furthermore, it is known that the problem of finding all Nash equilibria is a PPAD-complete problem even in the case of static games [33]. However, for practical purposes

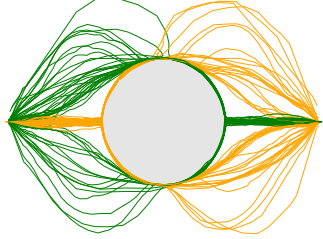


Fig. 2: When using MultiNash-PF on a difficult two agent trajectory game, we first employ an implicit particle filter to obtain coarse estimates of GNEs.

in multi-agent navigation, finding local solutions of (5) has proven to be enough for us.

The conventional approach to solving (5) relies on techniques such as interior point methods [24] or sequential quadratic programming [25]. Naively, the local solutions can be obtained by exhaustive initialization of random trajectories to an optimization solver, such as IPOPT [24], hoping to explore the solution space of local Nash equilibria. However, randomly exploring the nonconvex optimization landscape via gradient-based methods is computationally prohibitive and inefficient, as the same local equilibria can be arrived at from multiple random initializations. To address this, we utilize a Bayesian inference approach in the following section to efficiently recover all identified minima of (5).

IV. IDENTIFYING LOCAL NASH EQUILIBRIA VIA BAYESIAN INFERENCE

In this section, we propose our approach to solve (5) from a Bayesian inference perspective. We reformulate the optimal control problem (5) into an equivalent Bayesian inference problem by utilizing the reference trajectory and constraint violations as virtual measurements that provide evidence for the optimal inference of the system trajectory in (5). To this end, we first reformulate problem (5) by considering soft-constraints and introducing auxiliary variables $y_{x,t}$ and $y_{g,t}$ as:

$$\begin{aligned} \min_{\{v_t, w_t, \eta_t\}_{t=0}^{\tau}} & \|v_{\tau}\|_{Q_{\tau}}^2 + \sum_{t=0}^{\tau-1} \|v_t\|_Q^2 + \sum_{t=0}^{\tau} \left(\|w_t\|_R^2 + \|\eta_t\|_{Q_{\eta}}^2 \right), \\ \text{s.t. } & \begin{bmatrix} x_{t+1} \\ u_{t+1} \end{bmatrix} = \begin{bmatrix} f(x_t, u_t) \\ 0_m \end{bmatrix} + \begin{bmatrix} 0_n \\ w_t \end{bmatrix}, \\ & \begin{bmatrix} y_{x,t} \\ y_{g,t} \end{bmatrix} = \begin{bmatrix} x_t \\ \psi(g(x_t, u_t)) \end{bmatrix} + \begin{bmatrix} v_t \\ \eta_t \end{bmatrix}, \\ & \begin{bmatrix} x_0 \\ u_0 \end{bmatrix} = \begin{bmatrix} \hat{x}_0 \\ w_{t-1} \end{bmatrix}, \quad 0 \leq t \leq \tau, \end{aligned} \quad (7)$$

where v_t , w_t , and η_t are bounded disturbances. The weight matrix $Q_{\eta} \in \mathbb{R}^{n_c \times n_c}$ quantifies the slackness in satisfying constraints. Further, the degree of constraint violation is captured by a barrier function $\psi(\cdot, \cdot)$, which is defined as

$$\psi(g(x_t, u_t)) = \frac{1}{\alpha} \ln(1 + \exp(g(x_t, u_t))), \quad (8)$$

where α is a parameter that tunes the strictness of constraint enforcement.

A direct attempt at solving (7) using traditional gradient-based methods poses a similar computational burden in identifying all of the local equilibria compared to problem (5). However, the above connection between (5) and the moving horizon estimation problem (7) highlights the possibility to view the problem from a Bayesian inference perspective. To this end, we construct the following virtual state-space model from (7) as

$$\bar{x}_{t+1} = \bar{f}(\bar{x}_t) + \bar{w}_t, \quad \bar{y}_t = \bar{h}(\bar{x}_t) + \bar{v}_t, \quad (9)$$

where

$$\begin{aligned} \bar{x}_t &= \begin{bmatrix} x_t \\ u_t \end{bmatrix}, \quad \bar{y}_t = \begin{bmatrix} y_{x,t} \\ y_{g,t} \end{bmatrix}, \quad \bar{w}_t = \begin{bmatrix} 0_n \\ w_t \end{bmatrix}, \\ \bar{v}_t &= \begin{bmatrix} v_t \\ \eta_t \end{bmatrix}, \quad \bar{f}(\bar{x}_t) = \begin{bmatrix} f(x_t, u_t) \\ 0_m \end{bmatrix}, \quad \bar{h}(\bar{x}_t) = \begin{bmatrix} x_t \\ \psi(g(x_t, u_t)) \end{bmatrix}, \end{aligned}$$

where we relax \bar{w}_t and \bar{v}_t for $0 \leq t \leq \tau$ to be stochastic disturbances modeled as Gaussian-distributed random variables with density

$$\bar{v}_t \sim \mathcal{N}(0_{n+c}, \bar{Q}), \quad \bar{v}_{\tau} \sim \mathcal{N}(0_{n+c}, \bar{Q}_{\tau}), \quad \bar{w}_t \sim \mathcal{N}(0_{n+m}, \bar{R}),$$

with $\bar{Q} := \text{blkdiag}(Q^{-1}, Q_{\eta}^{-1})$, $\bar{Q}_{\tau} := \text{blkdiag}(Q_{\tau}^{-1}, Q_{\eta}^{-1})$, $\bar{R} := \text{blkdiag}(0_{n \times n}, R^{-1})$. The state estimation relevant to (9) is to estimate the state \bar{x}_t given the measurements \bar{y}_t . The value of the virtual measurements must be set in a way that steers the inference problem to have the same optima as in problem (5). We achieve this by noting that $y_{x,t}$ is a measurement value used to correct the state estimate of x_t towards the reference \hat{x}_t while $y_{g,t}$ is to satisfy constraints through (8). Observing that the barrier function in (8) outputs zero when the constraints are satisfied, we set the virtual measurement for the barrier function to be equal to 0_c . Hence, the virtual measurement that will drive \bar{x}_t towards optimality takes the value

$$\bar{y}_t = \begin{bmatrix} \hat{x}_t \\ 0_c \end{bmatrix}, \quad 0 \leq t \leq \tau.$$

The Bayesian inference problem pertaining to (9) is one that characterize the conditional distribution $p(\bar{x}_{0:\tau} | \bar{y}_{0:\tau})$. In the following lemma, we show that an equivalence holds between a posteriori estimate of $p(\bar{x}_{0:\tau} | \bar{y}_{0:\tau})$ and (5).

Lemma 1. *Assuming independence between the noise vectors \bar{v}_t and \bar{w}_t in (9), the problem in (5) has the same optima as*

$$\bar{x}_{0:\tau}^* = \arg \max_{\bar{x}_{0:\tau}} \log p(\bar{x}_{0:\tau} | \bar{y}_{0:\tau}).$$

We refer the interested reader to [14, Thm. 1] for the proof. The above lemma implies that the local GNEs in (5) translate to multiple local maxima of $p(\bar{x}_{0:\tau} | \bar{y}_{0:\tau})$. Hence, the Bayesian inference problem for (9) involves characterizing the multi-modal PDF $p(\bar{x}_{0:\tau} | \bar{y}_{0:\tau})$. Generally, state estimation of a multi-modal PDF does not admit closed-form solutions [34]. Hence, we resort to approximate solutions. A powerful approach is to use Monte Carlo methods that empirically approximate the distribution via a set of J particles as

$$p(\bar{x}_{0:\tau} | \bar{y}_{0:\tau}) \approx \sum_{j=1}^J w_j^j \delta(x_{0:\tau} - x_{0:\tau}^j), \quad (10)$$

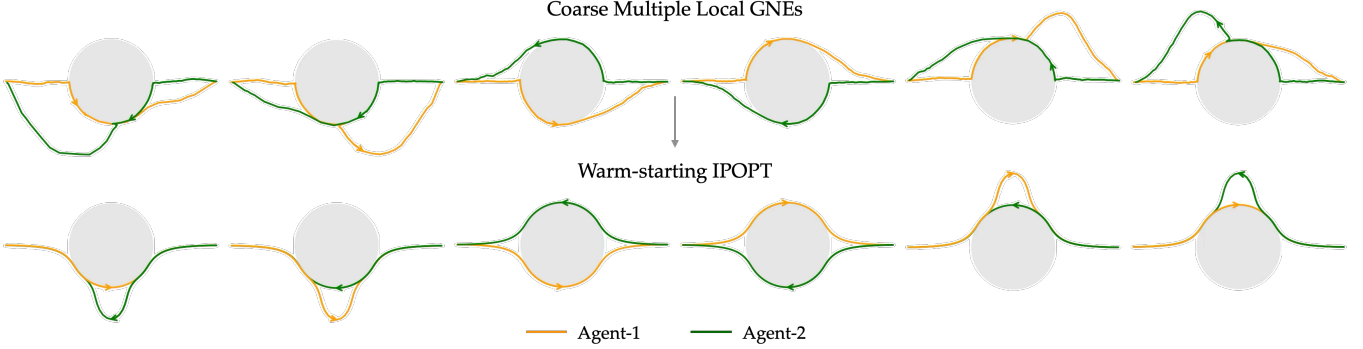


Fig. 3: MultiNash-PF identifies all the local GNE trajectories for a challenging two-agent trajectory game where two agents swapped positions while avoiding an obstacle. In this scenario, the obstacle radius is greater than the collision avoidance radius of the two agents, leading to the discovery of 6 distinct Nash equilibria. MultiNash-PF effectively obtains coarse estimates of local GNEs through implicit particle filtering, which are then refined using IPOPT to obtain local GNEs.

where $\delta(\cdot)$ is the Dirac delta function and w_τ^i is the weight assigned to a sample trajectory $\bar{x}_{0:\tau}^i$ for $j = 1, \dots, J$. It is important to note that, in our setting, each particle represents a complete trajectory.

To achieve the approximation in (10), we employ the implicit particle filter in [31] due to the twofold benefit it holds. First, as suggested in Lemma 1, the local maxima (i.e., high-probability regions) of $p(\bar{x}_{0:\tau} | \bar{y}_{0:\tau})$ correspond to the local GNEs. Hence, focusing our sampling efforts towards these high-probability regions can reduce the number of required samples for the approximation in (10). This approach aligns with the principle of implicit importance sampling, whose objective is to build a mapping that draws particles from the high-probability regions of the filtering distribution in (10). The implicit particle filter mitigates the particle degeneracy problem that pertains to particle filters by focusing the samples on the high-probability regions, which results in samples with large enough weights that are less prone to degeneration. Therefore, the implicit particle filter can often be deployed without requiring a resampling step [31], thereby resulting in smoother approximated trajectories, although occasional resampling may still be required.

We leverage the Markovian property of the virtual system (9) to recursively approximate (10) using Bayes' rule:

$$p(\bar{x}_{0:t} | \bar{y}_{0:t}) = p(\bar{y}_t | \bar{x}_t)p(\bar{x}_t | \bar{x}_{t-1})p(\bar{x}_{0:t-1} | \bar{y}_{0:t-1}), \quad (11)$$

for $0 \leq t \leq \tau$. This indicates that given the particle \bar{x}_{t-1}^j from the prior distribution $p(\bar{x}_{0:t-1} | \bar{y}_{0:t-1})$, we can obtain \bar{x}_t^j . As shown in [31], we use implicit importance sampling and identify an implicit mapping to sample from high probability regions of (11). The implicit map is constructed by considering sampling from a reference random vector ξ_t with density $p(\gamma_t)$ and mapping it to high probability regions of $p(x_{0:\tau} | y_{0:\tau})$, such that a sample γ_t^i is mapped to x_t^i . The mapping connects the highly probable regions of $p(\xi)$ to $p(x_{0:\tau} | y_{0:\tau})$ by letting

$$F(x_t^i) - \min F(x_t^i) = G(\gamma_t^i) - \min G(\gamma_t^i), \quad (12)$$

where $F(x_t^i) = -\log(p(x_t^i | y_{1:t}))$ and $G(\gamma_t^i) = -\log(p(\gamma_t^i))$. Finding an explicit solution to (12) is com-

putationally intractable due to the involved nonconvex optimization. To bypass this computational challenge, we employ a local Gaussian approximation around \bar{x}_{t-1}^j such that

$$p(\bar{x}_t^j | \bar{y}_{0:t}) \sim \mathcal{N}(\hat{m}_t^j, \hat{\Sigma}_t^{x,j}),$$

where \hat{m}_t^j and $\hat{\Sigma}_t^{x,j}$ are the mean and covariance of \bar{x}_t^j , respectively. These quantities can be approximated recursively using an Unscented Kalman filter (UKF) [35] for all $j = 1, \dots, N$. Then, the implicit map can be computed in closed form as

$$\bar{x}_t^j = \hat{m}_t^j + \sqrt{\hat{\Sigma}_t^{x,j}} \gamma_t^j,$$

where γ_t^j is a sample from $p(\gamma_t) \sim \mathcal{N}(0, I_n)$ and I_n denotes the identity matrix of size n .

We repeat this process until $t = \tau$ for each particle to obtain the set of trajectories $\{\bar{x}_{0:\tau}^j\}_{j=1}^J$, which will include the coarse estimates of local GNEs. This completes the unscented implicit particle filter, which identifies the coarse estimates of multiple local Nash equilibria in (5).

In the last step, we extract local equilibria from $\{x_{0:\tau}^j\}_{j=1}^J$. As viewed in Fig. 2, the particle set contains multiple trajectories for each GNE. Therefore, to isolate the GNE trajectories, we use a clustering method to aggregate the particles close to each other in one cluster. We leverage methods such as hierarchical clustering [36] or DBSCAN [37] for clustering purposes. It should be noted that clustering methods require a metric to compute distances between the data points. We use Fréchet distance [38] as our metric to compute distances between the trajectories. The clustering of trajectories will result in one cluster for each GNE. For each cluster, we compute the average trajectory which serves as an initial guess for the IPOPT solver. The solver then refines this initial guess by minimizing (5), ultimately converging to a precise local GNE. The algorithmic steps of the proposed *MultiNash-PF* are provided in Algorithm 1.

V. NUMERICAL SIMULATIONS

To showcase the capabilities of our method, we take motivation from real-life highway scenarios. We first consider an interaction between two agents moving toward each other

Algorithm 1 MultiNash-PF: Multiple local GNEs based on particle filter

- 1: Formulate the constrained dynamic potential game (5)
- 2: Setup the virtual model (9)
- 3: Perform unscented implicit particle filtering as follows:
- 3: Initialize the particles: \bar{x}_0^j , $\hat{\Sigma}_0^{x,j}$, and w_0^j for $j = 1, \dots, J$
- 4: Employ Algorithm-1 from [31] combined with UKF to obtain coarse solutions, $\{x_{0:\tau}\}_{j=1}^J$.
- 5: Extract trajectories through clustering from $\{x_{0:\tau}\}_{j=1}^J$ and warm start IPOPT solver to obtain the local GNEs $\{x_{0:\tau}^{i*}, u_{0:\tau}^{i*}\}_{i=1}^N$ of \mathcal{G} .

as shown in Fig 4. We consider the following discrete-time unicycle dynamics to model each agent $i \in \{1, 2\}$:

$$\begin{aligned} p_{t+1}^i &= p_t^i + \Delta t \cdot \nu_t^i \cos \theta_t^i, \quad q_{t+1}^i = q_t^i + \Delta t \cdot \nu_t^i \sin \theta_t^i \\ \theta_{t+1}^i &= \theta_t^i + \Delta t \cdot \omega_t^i, \quad \nu_{t+1}^i = \nu_t^i + \Delta \nu_t^i, \quad \omega_{t+1}^i = \omega_t^i + \Delta \omega_t^i, \end{aligned}$$

where Δt is the time-step size, p_t^i and q_t^i are x and y coordinates of the positions, θ_t^i is the heading angle from positive x-axis, ν_t^i is the linear velocity, and ω_t^i is the angular velocity of the agent i at time t . Further, $\Delta \nu_t^i$ is the change in linear velocity, and $\Delta \omega_t^i$ is the change in angular velocity of the agent i at time t , respectively. For each agent i , we denote the state vector x_t^i and the action vector u_t^i as follows

$$x_t^i = [p_t^i \quad q_t^i \quad \theta_t^i \quad \nu_t^i \quad \omega_t^i]^\top, \quad u_t^i = [\Delta \nu_t^i \quad \Delta \omega_t^i]^\top.$$

We formulate this scenario as a two-player game according to cost functions as described in (3). The reference trajectory for both agents is given as a straight line on the highway, starting from their initial position to their respective goal location. With $\hat{Q} = \text{blkdiag}(50, 10, 5, 5, 2)$, the reference tracking and control effort cost matrices are set as

$$Q^i = 0.6\hat{Q}, \quad Q_\tau^i = 100\hat{Q}, \quad R^i = \text{diag}(8, 4). \quad (13)$$

for $i \in \{1, 2\}$. In addition, the agents are subject to the constraint of avoiding collision with each other, which we define as

$$g_c(x_t, u_t) := -d(x_t^1, x_t^2) + r_{\text{col}} \leq 0, \quad (14)$$

where $d(x_t^1, x_t^2)$ is the Euclidean distance between the two agents and $r_{\text{col}} := 3m$ is the collision avoidance radius between the two agents.

With this setup, we employ MultiNash-PF from Algorithm 1 to efficiently capture the multi-modality in the solution space and then extract the solutions using hierarchical clustering [36] to provide a warm start trajectory to IPOPT [24] solver to recover different local GNEs. We use the Julia programming language and utilize the JuMP [39] library to solve the game using the IPOPT solver. The results of our method are provided in Fig 4. As we can see, the presence of two agents and collision avoidance constraints induces two different possible GNEs. Either both agents will yield to their right, or they will yield to their left to avoid collision. As shown in Fig 4, our method can recover both equilibria.

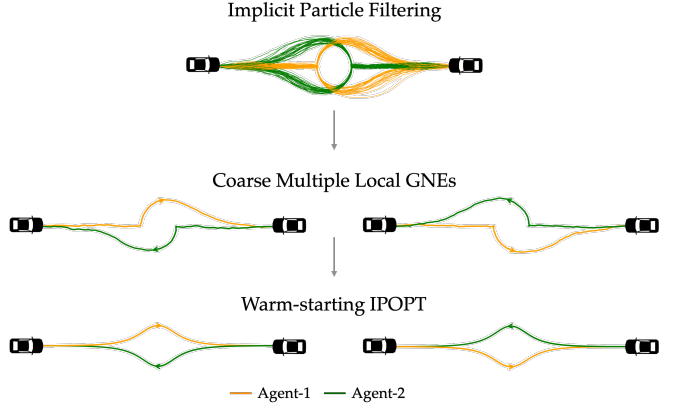
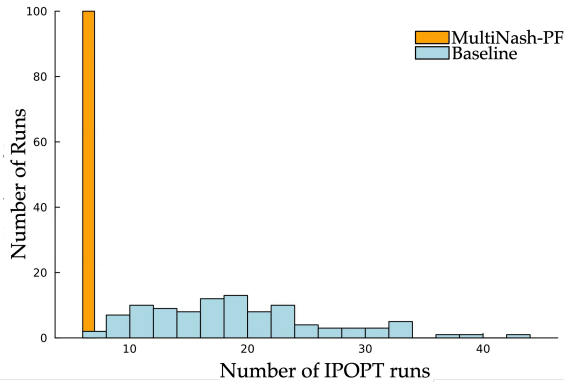


Fig. 4: The Nash equilibrium trajectories found by *MultiNash-PF* when two unicycle agents change their positions. First, we use the implicit particle filter to discover the coarse estimates of two different equilibria, and then utilize them as a warm start for IPOPT to obtain the two Nash equilibrium trajectories.

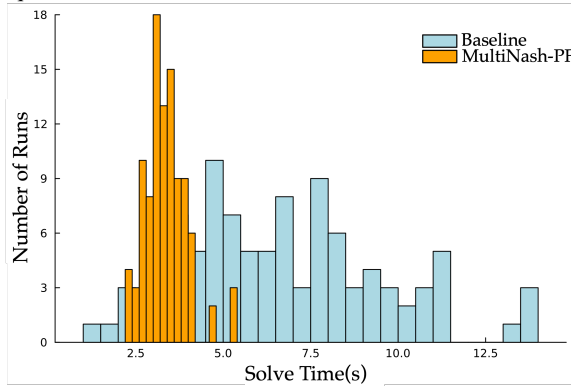
Next, we consider a more complicated scenario in which two agents aim to exchange their positions while avoiding an obstacle of radius $r_{\text{obs}} = 4m$ located at the midpoint of the two agents. Note that the radius of the obstacle is larger than the collision avoidance radius of the two agents.

We consider the same setup as before. In this example, in addition to (14), the constraints for this game will include both agents avoiding the obstacle $g_o^i(x_t, u_t) := [-d(x_t^i, x_{\text{obs}}) + r_{\text{obs}}]$ for $i = 1, 2$ where x_{obs} is the location of the obstacle. We also assume that we have constraints on the control bounds $g_b(x_t, u_t) = [-\nu_t^1, -\nu_t^2, |\nu_t^1| - u_b^1, |\nu_t^2| - u_b^2]$, where u_b^1 and u_b^2 are controlled action bounds for agents 1 and 2, respectively. We write the combined constraints as $g(x_t, u_t) := [g_c \quad g_o^1 \quad g_o^2 \quad g_b]^\top \leq 0$. We choose the values of control input bounds to be $u_b^1 = u_b^2 = [0.15, 0.75]^\top$. This setup induces multitudes of local equilibria. Two trivial local equilibria are when the two agents pass each other through opposite sides of the obstacle. However, there exist four other nontrivial equilibria when both agents can go on the same side of the obstacle, and one of the agents can yield to the other one. It is challenging to recover all six equilibria without utilizing the capabilities of the implicit particle filter. We fixed $J = 50$ particles and obtained the solution trajectories using implicit particle filtering from Algorithm 1 described in Section IV. Upon performing simulation experiments with our method, we observe that MultiNash-PF can recover all six Nash equilibria as shown in Fig. 2 and Fig. 3. Please note that, while trajectories may overlap spatially, collisions are avoided because agents traverse those regions at different times, as enforced by the constraints in our optimization.

1) *Comparison with Baseline:* In order to compare the effectiveness of our method, we consider a baseline method. For the baseline, we directly initialize the IPOPT solver with random perturbations of reference trajectories and compute the resulting optimal solutions. The computation time of our method is a combination of the time used in implicit



(a) Histogram of the number of IPOPT runs required to obtain all six equilibria.



(b) Histogram of the solve time comparison of MultiNash-PF and the baseline.

Fig. 5: Comparison of MultiNash-PF with the baseline for the experiment shown in Fig. 3.

(a) For the baseline, the average number of IPOPT runs required to obtain all six different equilibria is 18.64 ± 7.57 , while for MultiNash-PF, this is always 6. MultiNash-PF requires 3 times fewer IPOPT runs. (b) MultiNash-PF reduces the solve time by about 50% compared to the baseline while giving a much lower variance on the solve time.

particle filtering and the time used by IPOPT to obtain all the different equilibria given warm starting from filtering.

For the baseline, we randomly initialize the IPOPT solver until we recover all 6 different equilibria. We repeat this experiment for 100 different Monte Carlo runs. We observe that it requires, on average, 18.64 ± 7.57 random initializations of IPOPT to obtain all six different equilibria using the baseline approach. However, with our method, the number of IPOPT runs required is always six because we always obtain all six modes of equilibria from implicit particle filtering. A histogram of the number of IPOPT runs required for obtaining all six equilibria is plotted in Fig. 5a.

Furthermore, the solve time to recover all 6 different Nash equilibria for the baseline is 6.71 ± 2.83 s, while for MultiNash-PF, the solve time is 3.36 ± 0.59 s. Our method results in a solve-time reduction of 50% compared to the baseline while giving a much lower variance on the solve time. A histogram of the solve times of the baseline compared to our method is plotted in Fig. 5b. As explained earlier, our method's solve time is a combination of the

time used in implicit particle filtering and the time used by IPOPT. We observe that the time required for implicit particle filtering over 100 Monte Carlo runs is 0.37 ± 0.072 s while the time used by IPOPT to obtain the final solutions is 2.99 ± 0.57 s. Therefore, in our MultiNash-PF, the time used by implicit particle filtering is 11% of the total solve time, which shows that filtering is very efficient in exploring the solution space of local Nash equilibria.

VI. HARDWARE EXPERIMENT

Finally, we conduct a hardware experiment where a human and a robot exchange their positions as shown in Fig. 1. We perform these experiments using a TurtleBot 4, which is a ground robot with unicycle dynamics. We assume that the human also follows unicycle dynamics. The collision avoidance constraint between the TurtleBot and the human is assumed to be the same as that of (14). We use the Vicon motion capture system to measure the current position of both the robot and the human.

Similar as shown in Fig. 4, two GNEs may exist, which will correspond to two different modes of interactions. Namely, *yield-right equilibrium* when the human and robot yield to their right and *yield-left equilibrium* when they yield to their left. For the robot to safely navigate around the human without collision, the robot needs to be aware of both the GNEs and needs to be able to determine which GNE the human chooses. Using MultiNash-PF, the robot first uses an implicit particle filter to precompute the coarse estimates of the two different equilibria and then utilizes them as a warm start for IPOPT to obtain two modes of interaction. We assume that the interaction happens over $T = 10$ s. Then, similar to [11], the robot uses a potential function based game-theoretic planner in a model-predictive fashion with a planning horizon of 5s and $\Delta t = 0.1$ s to plan its motion.

The robot faces two precomputed choices of GNEs to follow recovered from the MultiNash-PF. At any given time t of planning, the robot computes the Fréchet distance [38] between the trajectory exhibited by the human so far and the human's trajectory in both the computed GNEs. Let the distances of the human trajectory from both the GNEs be denoted by d_1 and d_2 , respectively. The robot keeps an uncertainty on the GNE that the human chooses until $|d_1 - d_2| > d^*$ where d^* is a pre-specified threshold. For example, in Fig. 1, at $t = 2$, the values of d_1 and d_2 are almost identical, which indicates that the human has not chosen their mode of interaction. Whenever $|d_1 - d_2| > d^*$ occurs, the robot becomes certain of the mode of interaction followed by the human. Then, the robot follows the GNE corresponding to $\arg \min_{i \in \{1,2\}} \{d_i\}$. For example, in Fig. 1, at $t = 4$, the Fréchet distance of the human from its yield-left equilibrium trajectory is very high, while for the yield-left equilibrium, the Fréchet distance is low, indicating that the human has chosen the yield-right equilibrium. Using our method, the robot autonomously identifies this mode, moves accordingly, and reaches its goal location while successfully avoiding collision with the human.

We ran 10 different trials, and each time, we asked the human to either yield to their right or left randomly. Our algorithm was able to successfully compute both modes and identify the mode that the human was following. Using our algorithm, the robot was able to successfully avoid collision with the human in real-time and reach its goal location in all 10 runs.

VII. CONCLUSION

In this work, we introduced MultiNash-PF, a novel algorithm for efficiently computing multiple interaction modes. By leveraging potential game theory and implicit particle filtering, MultiNash-PF efficiently identifies coarse estimates of interaction modes, which are then refined using optimization solvers to obtain distinct interaction modes. Our numerical simulations demonstrate that MultiNash-PF significantly reduces computation time by up to 50% compared to baseline methods, while effectively capturing the multimodal nature of multi-agent interactions. Furthermore, our real-world human-robot interaction experiments highlight the algorithm's ability to reason about multiple interaction modes and resolve conflicts in real-time.

REFERENCES

- [1] R. Alterman and A. Garland, "Convention in joint activity," *Cognitive Science*, vol. 25, no. 4, pp. 611–657, 2001.
- [2] L. Peters, D. Fridovich-Keil, C. J. Tomlin, and Z. N. Sunberg, "Inference-based strategy alignment for general-sum differential games," *arXiv preprint arXiv:2002.04354[cs.RO]*, 2020.
- [3] J. Im, Y. Yu, D. Fridovich-Keil, and U. Topcu, "Coordination in noncooperative multiplayer matrix games via reduced rank correlated equilibria," *arXiv preprint arXiv:2403.10384[cs.GT]*, 2024.
- [4] T. Başar and G. J. Olsder, *Dynamic noncooperative game theory*. SIAM, 1998.
- [5] G. Galati, S. Primatesta, S. Grammatico, S. Macrì, and A. Rizzo, "Game theoretical trajectory planning enhances social acceptability of robots by humans," *Scientific Reports*, vol. 12, no. 1, p. 21976, 2022.
- [6] D. Fridovich-Keil, E. Ratner, L. Peters, A. D. Dragan, and C. J. Tomlin, "Efficient iterative linear-quadratic approximations for nonlinear multi-player general-sum differential games," in *2020 IEEE International Conference on Robotics and Automation (ICRA)*, pp. 1475–1481, IEEE, 2020.
- [7] D. Sadigh, S. Sastry, S. A. Seshia, and A. D. Dragan, "Planning for autonomous cars that leverage effects on human actions," in *Robotics: Science and systems*, vol. 2, pp. 1–9, Ann Arbor, MI, USA, 2016.
- [8] M. Bhatt and N. Mehr, "Strategic decision-making in multi-agent domains: A weighted potential dynamic game approach," *arXiv preprint arXiv:2308.05876*, 2023.
- [9] A. Dreves and M. Gerds, "A generalized Nash equilibrium approach for optimal control problems of autonomous cars," *Optimal Control Applications and Methods*, vol. 39, no. 1, pp. 326–342, 2018.
- [10] M. Wang, N. Mehr, A. Gaidon, and M. Schwager, "Game-theoretic planning for risk-aware interactive agents," in *2020 IEEE/RSJ International Conference on Intelligent Robots and Systems (IROS)*, pp. 6998–7005, IEEE, 2020.
- [11] M. Bhatt, Y. Jia, and N. Mehr, "Efficient constrained multi-agent trajectory optimization using dynamic potential games," in *2023 IEEE/RSJ International Conference on Intelligent Robots and Systems (IROS)*, pp. 7303–7310, IEEE, 2023.
- [12] Y. Jia, M. Bhatt, and N. Mehr, "Rapid: Autonomous multi-agent racing using constrained potential dynamic games," in *2023 European Control Conference (ECC)*, pp. 1–8, IEEE, 2023.
- [13] S. Zazo, S. V. Macua, M. Sánchez-Fernández, and J. Zazo, "Dynamic potential games with constraints: Fundamentals and applications in communications," *IEEE Transactions on Signal Processing*, vol. 64, no. 14, pp. 3806–3821, 2016.
- [14] I. Askari, X. Tu, S. Zeng, and H. Fang, "Model predictive inferential control of neural state-space models for autonomous vehicle motion planning," *arXiv preprint arXiv:2310.08045*, 2023.
- [15] S. M. LaValle, "Robot motion planning: A game-theoretic foundation," *Algorithmica*, vol. 26, pp. 430–465, 2000.
- [16] A. Liniger and J. Lygeros, "A noncooperative game approach to autonomous racing," *IEEE Transactions on Control Systems Technology*, vol. 28, no. 3, pp. 884–897, 2019.
- [17] R. Spica, E. Cristofalo, Z. Wang, E. Montijano, and M. Schwager, "A real-time game theoretic planner for autonomous two-player drone racing," *IEEE Transactions on Robotics*, vol. 36, no. 5, pp. 1389–1403, 2020.
- [18] M. Wang, Z. Wang, J. Talbot, J. C. Gerdes, and M. Schwager, "Game theoretic planning for self-driving cars in competitive scenarios," in *Robotics: Science and Systems*, 2019.
- [19] N. Mehr, M. Wang, M. Bhatt, and M. Schwager, "Maximum-entropy multi-agent dynamic games: Forward and inverse solutions," *IEEE transactions on robotics*, vol. 39, no. 3, pp. 1801–1815, 2023.
- [20] S. Le Cleac'h, M. Schwager, and Z. Manchester, "Algemes: a fast augmented lagrangian solver for constrained dynamic games," *Autonomous Robots*, vol. 46, no. 1, pp. 201–215, 2022.
- [21] T. Kavuncu, A. Yaraneri, and N. Mehr, "Potential iLQR: A potential-minimizing controller for planning multi-agent interactive trajectories," *arXiv preprint arXiv:2107.04926*, 2021.
- [22] Z. Williams, J. Chen, and N. Mehr, "Distributed potential ilqr: Scalable game-theoretic trajectory planning for multi-agent interactions," in *2023 IEEE International Conference on Robotics and Automation (ICRA)*, pp. 01–07, 2023.
- [23] M. Bhatt, Y. Jia, and N. Mehr, "Strategic decision-making in multi-agent domains: A weighted constrained potential dynamic game approach," *IEEE Transactions on Robotics*, 2025.
- [24] A. Wächter and L. T. Biegler, "On the implementation of an interior-point filter line-search algorithm for large-scale nonlinear programming," *Mathematical Programming*, vol. 106, no. 1, pp. 25–57, 2006.
- [25] P. T. Boggs and J. W. Tolle, "Sequential quadratic programming," *Acta numerica*, vol. 4, pp. 1–51, 1995.
- [26] I. Askari, A. Vaziri, X. Tu, S. Zeng, and H. Fang, "Model predictive inferential control of neural state-space models for autonomous vehicle motion planning," *IEEE Transactions on Robotics*, vol. 41, pp. 3202–3222, 2025.
- [27] I. Askari, S. Zeng, and H. Fang, "Nonlinear model predictive control based on constraint-aware particle filtering/smoothing," in *2021 American Control Conference (ACC)*, pp. 3532–3537, IEEE, 2021.
- [28] I. Askari, B. Badnava, T. Woodruff, S. Zeng, and H. Fang, "Sampling-based nonlinear MPC of neural network dynamics with application to autonomous vehicle motion planning," in *2022 American Control Conference (ACC)*, pp. 2084–2090, IEEE, 2022.
- [29] A. Doucet, N. De Freitas, N. J. Gordon, *et al.*, *Sequential Monte Carlo methods in practice*, vol. 1. Springer, 2001.
- [30] S. Särkkä and L. Svensson, *Bayesian filtering and smoothing*, vol. 17. Cambridge university press, 2023.
- [31] I. Askari, M. A. Haile, X. Tu, and H. Fang, "Implicit particle filtering via a bank of nonlinear Kalman filters," *Automatica*, vol. 145, p. 110469, 2022.
- [32] I. Askari, A. Vaziri, X. Tu, S. Zeng, and H. Fang, "Model predictive inferential control of neural state-space models for autonomous vehicle motion planning," *IEEE Transactions on Robotics*, 2025.
- [33] C. Daskalakis, P. W. Goldberg, and C. H. Papadimitriou, "The complexity of computing a Nash equilibrium," *Communications of the ACM*, vol. 52, no. 2, pp. 89–97, 2009.
- [34] S. Särkkä, *Bayesian Filtering and Smoothing*. Institute of Mathematical Statistics Textbooks, 2013.
- [35] E. A. Wan and R. Van Der Merwe, "The unscented kalman filter for nonlinear estimation," in *Proceedings of the IEEE 2000 adaptive systems for signal processing, communications, and control symposium (Cat. No. 00EX373)*, pp. 153–158, Ieee, 2000.
- [36] F. Murtagh and P. Contreras, "Algorithms for hierarchical clustering: an overview," *Wiley Interdisciplinary Reviews: Data Mining and Knowledge Discovery*, vol. 2, no. 1, pp. 86–97, 2012.
- [37] M. Ester, H.-P. Kriegel, J. Sander, X. Xu, *et al.*, "A density-based algorithm for discovering clusters in large spatial databases with noise," in *kdd*, vol. 96, pp. 226–231, 1996.
- [38] T. Eiter and H. Mannila, "Computing discrete fréchet distance," 1994.
- [39] I. Dunning, J. Huchette, and M. Lubin, "Jump: A modeling language for mathematical optimization," *SIAM review*, vol. 59, no. 2, pp. 295–320, 2017.